Heliyon 10 (2024) e40311

Contents lists available at ScienceDirect

Heliyon

journal homepage: www.cell.com/heliyon

Research article

Localized discrete and asymmetric dark-bright soliton-like modes as nonlinear dynamics in microtubules

Remi Jean Noumana Issokolo [a,b], Serges Eric Mkam Tchouobiap [b,*], Fernand Naha Nzoupe [b,c]

[a] National Advanced School of Engineering of Yaounde, University of Yaounde I, P.O. Box 8390 Yaounde, Cameroon
[b] Laboratory of Research on Advanced Materials and Nonlinear Sciences, Department of Physics, Faculty of Science, University of Buea, P.O. Box 63, Buea, Cameroon
[c] Laboratory of Mechanics, Department of Physics, Faculty of Science, University of Yaounde I, P.O. Box 812, Yaounde, Cameroon

ARTICLE INFO

Keywords:
Microtubules
Improved *u*-model
Polyelectrolyte effect
Kink-like solutions
Discrete localized modes
Asymmetric dark and bright solitary waves

ABSTRACT

In the present work, we focus on the longitudinal model of microtubules (MTs) proposed by Satarić et al. (1993) [12], and that considers MT cells to have ferroelectric properties (behaviors) due to dipolar oscillations of dimers within MTs, i.e., a displacive ferrodistortive system of heterodimers in MTs and usually referred to as *u*-model of MTs. It has been shown that during the hydrolysis of guanosine 5'- triphosphate into guanosine 5'-diphosphate, the energy released is transferred along the MTs through kink-like solitons. Substantially, we propose to theoretically investigate the dynamic of MTs by intrinsically taking into account the effect of oriented molecules of polarized cytoplasmic water and enzymes surrounding the MT. In this regards, we introduce a cubic nonlinear term in the electric potential characterizing the polyelectrolyte features of MTs and show that in addition to the kink and anti-kink dynamics, asymmetrical bright and dark solitons, and discrete modes can also propagate along the MTs. These results are supported by numerical analysis. The investigation shows us that the nonlinear dynamics of MTs is strongly impacted by the intrinsic electric field, the polyelectrolyte and the viscous effects. Moreover, new solitonic dynamics and discrete solitary modes might aid in the discovery of novel microtubulin system phenomena.

1. Introduction

As well known, MTs which have been extensively investigated in the literature, both experimentally and theoretically, are major components of cytoskeletal biopolymers (protein), whose biological functions depend largely on their mechanical properties [1–9]. Indeed, in conjunction with actin and intermediate filaments, MTs yield both static and dynamic frameworks that preserve cell structures, and are implicated in or the triggers of some specific myocardial cell functions such as intracellular transport of motor proteins and organelles, force generation for motor proteins, regulation of contraction, cells proteins ion channel function, receptor recycling, cells division and movement, etc [10–17]. Thus, within the framework of various experimental techniques and theoretical

* Corresponding author.
E-mail addresses: remi.issokolo@univ-yaounde1.cm (R.J.N. Issokolo), mkam.tchouobiap@ubuea.cm (S.E. Mkam Tchouobiap), fernand.naha.nz@gmail.com (F. Naha Nzoupe).

https://doi.org/10.1016/j.heliyon.2024.e40311
Received 16 August 2023; Received in revised form 7 November 2024; Accepted 8 November 2024

Available online 14 November 2024

approaches [18–33], all eukaryotic cells have MTs; and their association with microfilaments and actin filaments form the cell's cytoskeleton which is a network of long protein fibers that compose the structural framework of the cell.

Microtubules are cylindrical-like assembly of a set of tubulin proteins through the formation of 13 longitudinal protofilaments (PFs) covering its cylindrical wall, that has an outer and inner radii of 25 nm and 15 nm, respectively, and each PF appears as a string of proteins composed of $\alpha - \beta$ tubulin heterodimers [1–8]. During the mechanism of formation of MTs, there is a continuous binding or conformational change of molecules of tubulin dimers caused by one tubulin monomer shifting its orientation by 29° off the dimer's vertical axis as a result of the hydrolysis of the guanosine 5'- triphosphate (GTP) and guanosine 5'-diphosphate (GDP) molecules [12–15,17,18], and accompanied by a continuous high consumption of energy, making this process dissipative as their self-organization is energy-intensive [9–11]. Based on their structural and functional characterization, MTs can therefore be thought of as reaction-diffusion systems, and as such they are very dynamic tubulin dimers' polymers associated in a chain-like manner [6,7,9–13].

Also, MTs appear as a good candidates for dynamic information processing since it was shown that the brain's storage, processing, and transduction of biological information are primarily or fundamentally controlled by neuronal MTs [2–6,14,21]. More specifically, there is evidence that the dynamic coupling of the cytoskeleton polymers, which is mediated by mechanical energy, could store and process information, and mechanical properties of MTs involving bending or buckling MTs are largely responsible of most of their biological functions [19–24]. Beside their mechanical role as a part of the cytoskeleton, MTs act as highways for several motor proteins, including kinesin and dynein, which travel along MTs for microtubule-based delivery of cargo molecules in- vivo to particular synapses and locations (sites) [2,25–29].

Among other things, MTs are known to undergo a tread-milling phenomenon [5,12–15,17–20]. In this regards, as far as their structure polarities are concerned with positive and negative ends, they undergo various activities of rapid polymerization due to their assembly in the positive (+) end, and depolymerization due to their disassembly in the negative (-) end [5,19,20]. Moreover, MTs control the internal organization of the cells and their shapes. They also undergo various activities such as the intracellular transport of biological materials, cellular mobility, cytoplasmic transport and mitosis [21,30]. Hence, it is still crucial to have a panoramic understanding of their mechanisms.

Indeed, taking into account the strong intrinsic nonlinear complex interactions in MTs such as their non-equilibrium dynamic has led to the development of mathematical models supported by theoretical analysis to understand the intrinsic properties and behaviors of the PFs. In this regards, following various purposes associated with the excitability and the propagation of nonlinear ionic waves in MTs, some theoretical studies have considered electrophysiological features of MTs, and modeled the MTs as an electric circuit with nonlinear resistance [31–33]. For example, an existing electrical model was upgraded to study the ionic currents propagating in narrow layer along MTs [32], while another electrical model was proposed and applied for the investigation of the amplification, infratrasmission and supratransmission of electrical signal in MTs [33]. For the later model, it was discovered that the system considerably increased the input signal's amplitude, validating some known experimental findings. In addition, considering the capability of the PFs to behave like an excitable structure, another electrical model was also proposed that encapsulate various excitability features of PFs, and the description of the developmental and informative processes taking place on the subcellular scale may be of significant relevance to the study, according to the hypothesis [31].

On the other hand, in various studies describing the MTs nonlinear dynamics, a well-known mathematical model based on the ferroelectric-like behavior of MTs is usually considered, namely the so-called u-model. The u-model, firstly introduced by Satarić et al. [12], and later on improved and used in various works [11,22,26–28], is mainly associated with the nonlinear dynamics of dimer dipoles in the ordered PF structures that covers the cylindrical walls of MTs. In fact, only one degree of freedom of dimer motion within the PF is assumed by the u-model, namely the longitudinal oscillations of dimers along the PFs aligned in directions parallel to the MT axes. Accordingly, the longitudinal displacement of a dimer dipole at a given point n, represented by the symbol u_n, is the only degree of freedom per dimer that the u-model takes into account, making it the oldest and most well-known nonlinear model to date for explaining complex dynamics of MTs. More specifically, the coordinate u_n is a projection of the top of the dimer on the direction of PF, and the u-model depends on an essential angular degree of freedom because of angular dipolar oscillations carried out by dimers within the MT [12,26,28]. The nearest adjacent approximation is utilized in this model, which has been the subject of much research, to describe the interaction between dimers that belong to the same PF and the fact that dimers are electric dipoles that reside in the field of other MT dipoles. Additionally, as in a series of models describing MT nonlinear dynamics, the first u-model and its improved versions [12,26,28], as well as the real longitudinal model [34], which take the longitudinal displacement coordinate for each dimer as the only degree of freedom, belong to the group of longitudinal models and, for the sake of simplicity, assume that the solvent is made up of water molecules. These dipolar molecules which function as a viscous medium to dampen out vibrations of the dimer dipoles, will have a significant impact on the long-range electrostatic energy between the dimers [12,25–28,34].

In this respect, the u-model generally considers the kinetic energy of each dimer, a harmonic potential energy of the chemical interaction between the neighboring dimers (nearest-neighbor) belonging to the same PF, a one-site potential energy representing the overall effect of the surrounding dimer dipoles on the dimer at that site and in the form of the widely known double-well potential of the ϕ^4-type, the energy of the dimer in the intrinsic electric field as linear electrical potential energy, and a viscosity force for the description of MTs dynamics [12,22,26–29,34]. Therefore, the induced equation takes into account substantially the effect of dispersion, viscous dissipation and nonlinearity, essentially necessary for the study of the energy propagation in MTs and the interesting assembly and disassembly mechanisms of polymerization and depolymerization processes of heterodimers in microtubulin systems. In addition, to solve the induced equation and to study the traveling wave solutions, a couple of powerful mathematical methods or procedures has been usually proposed, such as the standard procedure [12,35], the semi-discrete approximation method [11,22], the tangent hyperbolic function method (THFM) or tanh-expansion method [16,36,37], the extended THFM [38,39], the modified extended tanh-function method (METHFM) [26,39–42], the approach based on Jacobian elliptic functions [29,43], the factoriza-

tion method [28,44,45], the simplest equation method (SEM) which is the most general procedure [25,27,36,46], and its simplified variant called the modified simplest equation method (MSEM) [47], the exponential function procedure [48–50], the double and multiple exp-function methods [51,52] and the hyperbolic ansatz method [53], just to name a few. However, many of them share a series expansion of the solutions in terms of known functions in addition to the standard technique, the factorization approach, and the hyperbolic ansatz approach. Accordingly, by using these existing mathematical tools, various authors have proposed different solutions describing the dynamics of MTs in terms of tanh- and cotanh-functions [25,26,36,39,40], sech-function [11,22], and exp-function [12,18,49,50]. More importantly, Zeković et al. [29] showed the possibility of using Jacobi elliptic functions [29,43] to obtain analytical solutions for the given model, by presenting the link between Jacobi elliptic functions and hyperbolic functions [54,55].

Moreover, it is noteworthy to mention that it is also possible to expand the series in terms of unknown functions [56]. However, the fact that the function employed for the series expansion is unknown is a significant aspect (key component) of the series expansion unknown function method (SEUFM) which was proposed and implemented more recently [57]. Furthermore, it was shown that the solutions obtained using THFM and METHFM are special cases of those obtained using both SEUFM and SEM, and instead of obtaining a single physical solution it seems that SEUFM yields an endless number of solutions [57]. Subsequently, this is not particularly relevant to the physics of MTs, though, because all of them have the same physical meaning when it comes to nonlinear MT dynamics.

In the present study, we propose a modified u-model that describes the nonlinear dynamics of MTs by taking into account their polyelectrolyte features. Indeed, as oriented assembly of dipoles, it has been shown that many factors, including the stored mechanical energy, gravity, hydrodynamic flow, thermally induced vibrations, shape fluctuations, flow-induced vibrations and induced electromagnetic field, influence the energy propagation in MTs and their functions; particularly the extremely fascinating way in which they assemble (polymerization) and disassemble (depolymerization) via the tubulin dimers in PFs [12,16,58–64], as they act through the structured water molecules, the cytoplasmic water and enzymes surrounding the MT. In the same vein, considering the intrinsic electric field, as well as the ferroelectric properties of the dimer that are essential to propagation direction of the energy excitation from the hydrolysis [12,14], we propose to include a cubic term in the electric potential that account for the nonlinear intrinsic electric interactions in the cell. In order to proceed with the investigation and the analysis of the given mathematical model, we apply a method proposed by Samsonov [65,66] to carefully examine some features associated with the energy propagations in MTs. Through that method, we observe the propensity of MT's assembly to favor the emergence of various localized patterns including localized discrete modes, and asymmetrical bright and dark solitons, whose generation and evolution are influenced by the polarized solvent (water), the viscous force, and the cooperative nonlinear interaction of the intrinsic electric field. These solutions are obtained using exp-function, Jacobi elliptic functions, and Weierstrass $\wp$-function associated with Jacobi elliptic functions, through various transformations that can be found in various documents and textbooks [39,54,62,63,65–69].

The paper is organized as follows: In Section 2, we introduce the improved longitudinal u-model for MTs and briefly explain the theoretical framework and mathematical procedures necessary to derive the relevant dynamical equation of motion, the crucial differential equation, and the solutions of the nonlinear dynamical model. Section 3 focuses on the analyses and discussions of the obtained solutions, while in Section 4 we examine the stability analysis of the resulting solutions. Finally, concluding remarks are covered in Section 5.

2. Mathematical model and theoretical framework

2.1. Model formulation and equation of motion

Considering the dynamics of the heterodimers in the longitudinal direction expressed by the u-model, the nonlinear dynamical equation to describe the oscillations of MTs is presented by the system's Hamiltonian that has the form [12,26–28]:

$$H=\sum_{n=1}^{N}\left[\frac{m}{2}\dot{u}_n^2+\frac{K}{2}(u_{n+1}-u_n)^2+V_1(u_n)+V_2(u_n)\right], \tag{1}$$

where the overdot represents the first derivative with respect to time, m is the mass of the single dimer ($m=1,8\times10^{-22}$ kg), K stands for an effective intra-dimer stiffness parameter or dimer-dimer bonding interaction parameter within the same PF while N denotes the total number of single tubulin dimers that belong to the same PF, and the integer n indicates the location of the considered dimer in the PF [12,26–28]. Hence, it is obvious that the first term clearly represents the kinetic energy of the dimer at position n, while the second one is the energy of interaction between the dimers within the framework of the mean-field treatment, and where the nearest-neighbor approximation is also considered. Hence, this term characterizes the mean-field approximation for interactions between dimers while taking into account the nearest-neighbor approximation or the quasiharmonic vibrations of the dimers.

However, as an important part of the Hamiltonian and a source of nonlinearity is the potential energy connected to each dipole and represented by the final two terms. The first one is due to the overall effects (mechanochemical influences) of all surrounding tubulin dimers on the dimer dipole at a chosen site n, and of the polarized cytoplasmic water molecules and enzymes surrounding the MT; while the second one is induced by the nearly uniform intrinsic electric field generated by all other tubulin dimers, including the dimers belonging to neighboring PFs and the polarized cytoplasmic water. In addition, it is noteworthy that dimers are electric dipoles existing in the electric field of all other dipole dimers of the MT, including the dipoles belonging to the neighboring PFs (i.e., all other ones that do not belong to the same PF). Indeed, the presence of oriented molecules of cytoplasmic water and enzymes surrounding the MT was experimentally observed using electron microscopy technique [70], which imply their plausible participation

or responsibility in the nonlinear dynamics and stability of MTs which are crucial for biological systems, in several cellular activities, including growth and division, which are known to be necessary for the living state of MTs, and in numerous mechanisms or cellular processes such as information processing (the transfer and storage of information in brain microtubules) which are fundamental for understanding MT nonlinear dynamics [2,14,71]. Important in this respect, we also assume that an MT and the polarized cytoplasmic water around it induce an almost uniform intrinsic electric field parallel to its axis, and that the additional potential resulting from the internal electric field and the surrounding polarized water is nonlinear in nature for each dipole. Moreover, $V_1(u_n)$ is a generalized double-well potential of Φ^4-type that displays the overall effect of the surrounding dimers on a tubulin dipole at a given site n, and which is due to the ferroelectric (displacive ferrodistortive) behavior of MTs [5,12,22–26,63,72,73].

In addition, $V_2(u_n)$ is the additional potential energy associated with each dipole dimer, which is due to the intrinsic (internal) electric field generated by the MT [12,22,26,27], and to the surrounding polarized water and microtubule-associated proteins, responsible for interconnection of parallel-arrayed MTs in the microtubulin systems. These interconnections, together with MTs, appear to be in charge of a variety of cellular processes, including growth and division, which are vitally important for the living state [1,2,6,12,18]. Therefore, in the present analysis the potential energies $V_1(u_n)$ and $V_2(u_n)$ are expressed as:

$$V_1(u_n) = \frac{1}{4} B u_n^4 - \frac{1}{2} A u_n^2, \qquad V_2(u_n) = -C u_n - \frac{1}{3} \epsilon u_n^3, \qquad C = q E, \tag{2}$$

where A, B and ϵ are positive model parameters to be determined or at least estimated, even though A is typically a linear function of the temperature [12] that generally change sign at an instability temperature T_c [15]; q represents the excess charge inside the dipole, and E is the uniform intrinsic electric field strength (magnitude) directed along the longitudinal axis of the MT cylinder, with $q > 0$, and $E > 0$.

It is important to precise that the intrinsic electric field E is induced by all dimers including the dimers from the neighboring PFs. Fig. 1 displays the potential energies $V_1(u_n)$ and $V_2(u_n)$ with and without the added (correction) term, and the combined potential energy $V_1(u_n) + V_2(u_n)$, yielding a non-symmetric double-well potential (W-potential). As the potential energy $V_1(u_n)$ takes into account quantum chemistry considerations through the chemical effect of all other dimers of the MT [24,63,73–76], its shape for an isolated single-dimer is depicted in Fig. 1(a), where it is evident that the potential $V_1(u_n)$ is a symmetric W-potential possessing two degenerated minima separated by a potential barrier. Fig. 1(b) presents the additional potential energy $V_{el}(u_n) = -q E u_n = V_2(u_n)|_{\epsilon=0}$, acquired by the dimer as an electric dipole and induced by the intrinsic electric field of the MT. It can be noticed that V_{el} which takes into account the intrinsic helicity of the MT, exhibits linear behavior because of the consistent uniform intrinsic electric field produced parallel to the MT axis [12,26,34].

More importantly, to correspond with the actual MT structure, MTs can be broadly recognized as oriented assemblies of dipole dimers [12,87]. Accordingly, it seems that the tubulin dipole dimers are capable of undergoing conformational changes inside PFs, which might spread along either single PFs or tiny clusters of PFs, and such cooperative conformations are responsible for quite important functions of MTs and cellular activities, especially during the polymerization (assembly) and depolymerization (disassembly) processes of MTs [7,16,20,76,77]. For example, the peeling apart of the curved PF fragments at the ends of MTs during disassembly is the consequence of such cooperative conformations [16,77]. Accordingly, Fig. 1(c) shows that $V_2(u_n)$ with $\epsilon \neq 0$ possesses local extrema which are likely responsible for the orientation towards the right or left of the symmetrical potential $V_1(u_n)$. The nonlinear character of $V_2(u_n)$ suggests beyond expectations that various excitation phenomena can be generated regarding the energy propagation within MTs, as can be seen in Fig. 1(c). To the best of our knowledge, the association of both potentials must result in the lifting of the degeneracy (breaking of symmetry), leading to a more realistic asymmetric W-potential, as shown in Fig. 1(d). Moreover, the profile of the combined potential defined as $V_1(u_n) + V_2(u_n)$ is presented in Fig. 1(d), allowing us to appreciate the impact of the parameter ϵ on the potential's asymmetry. Therefore, Fig. 1(d) presents in a clearcut way the asymmetric behavior of the combined potential as a non-symmetric function, with a right and a left minima, in accordance with the fact that the distribution of the dimers strongly suggests the plausibility of the two inclinations of the dimers, characteristics of the ferroelectric behavior and corresponding to the minima. In this regards, we observe that as ϵ increases, the bistable potential $V(u_n)$ gradually evolves into a state where its bistability character will be loosed. Such that, for a critical value of ϵ, $V(u_n)$ will no more be bistable.

At this level let us introduce generalized coordinates q_n and p_n defined as $q_n = u_n$, $p_n = m\dot{u}_n$. By using the Hamilton's equations of motion $\dot{p}_n = -\partial H/\partial q_n$ and $\dot{q}_n = \partial H/\partial p_n$ and applying a continuum approximation (long wavelength limit) $u_n(t) \to u(x,t)$, while eventually making a Taylor series expansion of terms $u_{n\pm1}$, i.e. [12,26],

$$u_{n\pm1} \to u \pm \frac{\partial u}{\partial x} l + \frac{1}{2} \frac{\partial^2 u}{\partial x^2} l^2, \tag{3}$$

where l is the dimers length, representing a period of one dimensional crystal lattice, Eq. (1) can be straightforwardly transformed into the following appropriate continuum dynamical equation of motion:

$$m\frac{\partial^2 u}{\partial t^2} - K l^2 \frac{\partial^2 u}{\partial x^2} + B u^3 - \epsilon u^2 - A u - qE + \gamma \frac{\partial u}{\partial t} = 0, \tag{4}$$

which is a nonlinear partial differential equation (PDE), and where in order to derive a realistic equation, the viscosity of the solvent manifested by the damping of dimers vibrations has been taken into consideration, through the introduction of a viscous force $F_v = -\gamma \frac{\partial u}{\partial t}$, with γ denoting the viscous (damping) coefficient [12,26].

As well-known, Eq. (4) can be further adequately transformed into an ordinary differential equation (ODE) by introducing a unified coordinate z along with a dimensionless function ψ defined as usual through the relations:

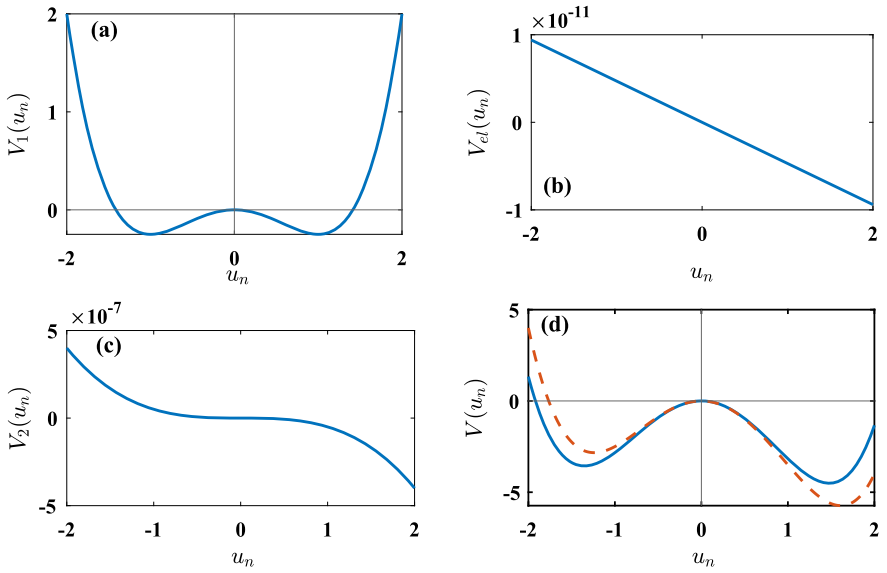

Fig. 1. Profiles of the well-known symmetric double-well potential energy of Φ^4-type $V_1(u_n)$(a), the additional potential energy potential $V_2(u_n)$ without additional term (b) (expressed here as V_{el}) and with additional term (c), and of the combined non-symmetric double-well potential energy $V(u_n) = V_1(u_n) + V_2(u_n)$ (d), associated with each dipole dimer as a function of the longitudinal displacement of a dimer at a given position n, u_n. The model parameters are selected as follows: (a) $A = 1.0$ N$[u_n]^{-1}$ and $B = 1.0$ N$[u_n]^{-3}$, $C = 4.7 \times 10^{-12}$ N; and: (b) $\epsilon = 0$ and (c) $\epsilon = 5.0 \times 10^{-8}$ N$[u_n]^{-2}$; (d) $A = 8.0$ N$[u_n]^{-1}$ and $B = 4.0$ N$[u_n]^{-3}$, $C = 4.7 \times 10^{-12}$ N, $\epsilon = 0.5$ N$[u_n]^{-2}$ (solid line) and $\epsilon = 1.5$ N$[u_n]^{-2}$ (dashed line). The unit of x-axis graduated by u_n is $[u_n]$ while the unit of y-axis is one N$[u_n]$.

$$z = kx - \omega t \qquad \text{and} \qquad u = \sqrt{\frac{A}{B}}\psi, \tag{5}$$

where k and ω are real constants denoting the wave number and the frequency, respectively, while the function $u = u(x,t) \equiv u(kx - \omega t) = u(z)$ is the traveling wave. Hence, z is the traveling wave variable and denotes the moving coordinate, while the dimensionless function $\psi = \psi(x,t) \equiv \psi(z)$ represents the elongation of the oscillating dimer at position x and at time t only through a unified variable z. Accordingly, by inserting the above suitable transformations given in Eq. (5) into Eq. (4) the following ODE is derived:

$$\alpha\psi'' - \rho\psi' + \psi^3 - \beta\psi^2 - \psi - \sigma = 0, \tag{6}$$

where the prime ($'$) sign denotes the first derivative with respect to the unified variable z, i.e., $\psi' = \frac{d\psi}{dz}$. Besides the following four dimensionless new parameters α, ρ, β and σ underpinning the physics of the relevant model as:

$$\alpha = \frac{mw^2 - Kl^2k^2}{A}, \qquad \rho = \frac{\gamma w}{A}, \qquad \beta = \frac{\epsilon}{B\sqrt{\frac{A}{B}}}, \qquad \sigma = \frac{qE}{A\sqrt{\frac{A}{B}}}. \tag{7}$$

Indeed, it is noteworthy that as expressed in Eq. (7), the parameter α accounts for the competitive interaction between the kinetic energy of the dimers and the relevant chemical bounds, while the parameter β accounts for the polyelectrolyte features of MTs. Likewise, the dimensionless parameters ρ and σ are proportional to the viscous force and electric field strength, respectively. All of these effects are very important as they are crucial for nonlinear dynamics and stability of MTs, and for understanding mechanisms such as dynamical information processing and energy transfer; and cellular activities and processes including mitosis, metabolism, cell growth and division, meiosis and transport of cellular cargo motor proteins in MTs [11–14,76,78].

2.2. Mathematical approach and analytical solutions

As well known, Eq. (6) is a nonlinear dispersive (even order term) and dissipative (odd order term) ODE and in the present study, we will use a mathematical approach proposed by Samsonov [65] to find explicit solutions of the above ODE. This method has the advantage to used simple transformations that transform Eq. (6) to an equation solvable using Jacobi elliptic and Weierstrass $\wp$-functions, without considering the Painleve properties [79] of Eq. (4). More interesting, and for the sake of simplicity, we first rewrite Eq. (6) as follows:

$$\psi'' - \mu_0\psi' - m_1\psi - m_2\psi^2 + m_3\psi^3 - m_0 = 0, \tag{8}$$

where the coefficients μ_0, m_0, m_1, m_2 and m_3 are defined as:

$$\mu_0 = \frac{\rho}{\alpha}, \ m_0 = \frac{\sigma}{\alpha}, \ m_1 = \frac{1}{\alpha}, \ m_2 = \frac{\beta}{\alpha}, \ m_3 = \frac{1}{\alpha}, \tag{9}$$

with the restriction (constraint) $\alpha \neq 0$. In this regards, according to the mathematical basis for our theoretical framework procedures and in order to practically address Eq. (8), it might be convenient to introduce new dimensionless functions. Thence, by considering and performing the following transformation:

$$\psi' = \frac{d\,\psi}{d\,z} = \frac{1}{\phi(\psi)}, \tag{10}$$

Eq. (8) is reduced to a dynamical first order ODE with respect to the new function ϕ of the form:

$$\phi' - \mu_0\phi^2 + (-m_1\,\psi - m_2\,\psi^2 + m_3\,\psi^3 - m_0)\,\phi^3 = 0. \tag{11}$$

However, it is noteworthy that the first order ODE given by Eq. (11) is not easily exploitable or solvable in order to obtain a possible solution to Eq. (8). For this purpose and to proceed further into our investigation, we perform a second transformation defined as:

$$\frac{\partial\eta}{\partial\xi} = \frac{1}{\xi\phi(\eta)}, \tag{12}$$

and insert it into Eq. (11), with the aim of transforming Eq. (11) into a second order ODE without a first-order derivative term. In this vein, before applying appropriate derivations and computations, we should keep in mind that: $\psi = \psi(z)$, $\phi = \phi(\psi)$, and $\eta = \eta(\xi)$ such that $\phi(\psi) = \phi[\psi(z)]$, and $\phi(\eta) = \phi[\eta(\xi)]$. Within the framework of the technique described in [65,66], we can straightforwardly obtain the following nonlinear evolution equation (i.e., a second order ODE in η):

$$\xi^2\frac{\partial^2\eta(\xi)}{\partial\xi^2} + \Gamma_3\eta^3 - \Gamma_2\eta^2 - \Gamma_1\eta - \Gamma_0 = 0, \tag{13}$$

where the different coefficients are defined as:

$$\Gamma_0 = \frac{\sigma}{\rho}, \qquad \Gamma_1 = \frac{\alpha}{\rho^2}, \qquad \Gamma_2 = \frac{\beta\alpha^2}{\rho^3}, \qquad \Gamma_3 = \frac{\alpha^3}{\rho^4}, \tag{14}$$

provided that $\rho \neq 0$, and where the functions $\psi(z)$ and $\eta(\xi)$ have to be determined. Here, Eq. (13) is of capital importance as it is the mathematical equation which is the basis of our analysis.

Before we proceed further into our investigation, it is useful to precise that the relation between $\psi(z)$ and $\eta(\xi)$ appears as an important point in the treatment. For this reason and for simplicity we have considered for convenience a linear relation between $\psi(z)$ and $\eta(\xi)$, and defined as [65,66]:

$$\eta = \int \mu_0\,d\psi, \tag{15}$$

which is one of the main transformation used to obtain Eq. (13). Indeed, Eq. (15) provides a link between the unknown function η and the original function ψ via the parameters of the system, which appear rather useful to transform Eq. (11) into a second order ODE with respect to the function η. Likewise, the integration of the transformation Eq. (15) leads to the relation $\eta = \mu_0\psi$ since μ_0 is a constant; such that $\frac{\partial\phi}{\partial\eta} = \frac{\partial\phi}{\partial\psi}\frac{\partial\psi}{\partial\eta} = \frac{1}{\mu_0}\frac{\partial\phi}{\partial\psi}$, and where the expression of the parameter μ_0 is given in Eq. (9). However, let us note that one of the major difficulties of this mathematical method lies in the choice of the appropriate ansatz, since the ansatz varies with the equation form. At this point, a solution of Eq. (13) for η can be constructed by assuming it to be of the form [65]:

$$\eta = a_0\delta^{\frac{p}{r}}\Phi(\delta) + \eta_0, \qquad \text{with} \qquad \delta = \xi^r. \tag{16}$$

Here of course, p and r, and the functions $\xi = \xi(z)$, $\delta = \delta(z)$ and $\Phi = \Phi(\delta)$ should also be determined, meanwhile a_0 and η_0 are arbitrary constants. In addition, we should also emphasize here that plugging the expression of the trial function $\eta = \eta(\xi)$ given in Eq. (16) into Eq. (13), brings about the following dynamical equation governing the dynamics of the microtubulin system:

$$\begin{aligned} &r^2a_0\delta^{\frac{p+2r}{r}}\Phi_{\delta\delta} + [2pr + r(r-1)]a_0\delta^{\frac{p+r}{r}}\Phi_\delta + \Gamma_3a_0^3\delta^{\frac{3p}{r}}\Phi^3 + (3\Gamma_3\eta_0 - \Gamma_2)a_0^2\delta^{\frac{2p}{r}}\Phi^2 \\ &+ [p(p-1) - \Gamma_1 - 2\Gamma_2\eta_0 + 3\Gamma_3\eta_0^2]a_0\delta^{\frac{p}{r}}\Phi - \Gamma_0 - \Gamma_1\eta_0 - \Gamma_2\eta_0^2 + \Gamma_3\eta_0^3 = 0, \end{aligned} \tag{17}$$

where subscript indexes δ and $\delta\delta$ denote the first and second derivatives with respect to δ, respectively, i.e., $\Phi_\delta = \frac{d\,\Phi}{d\,\delta}$ and $\Phi_{\delta\delta} = \frac{d^2\,\Phi}{d\,\delta^2}$. Hence, following the theoretical method explained above, the ansatz for the solution η must be consistent with the series expansion of the above equation in powers of the function $\Phi = \Phi(\delta)$, adopted in Eq. (16), and its derivatives [65,66,79]. Since, a_0, r, Γ_3, ξ and δ can not be zero, by eliminating the terms which consisting $\Phi_{\delta\delta}$ and Φ^3, when the corresponding coefficients of the other terms Φ^0, Φ^1, Φ^2 and Φ_δ are equated to zero, brings the following four equations:

$$\Phi^0 \ : -\Gamma_0 - \Gamma_1\eta_0 - \Gamma_2\eta_0^2 + \Gamma_3\eta_0^3 = 0, \tag{18}$$

$$\Phi^1 \ : p(p-1) - \Gamma_1 - 2\Gamma_2\eta_0 + 3\Gamma_3\eta_0^2 = 0, \tag{19}$$

$$\Phi^2 \ : 3\Gamma_3\eta_0 - \Gamma_2 = 0, \tag{20}$$

$$\Phi_\delta \ : 2p + r - 1 = 0. \tag{21}$$

Of central importance, let us note that the above system of equations induces only implicit relations between the parameters [65]. On the other hand, Eq. (20) is of physical interest, hence this equation will be explicitly exploited in the rest of our study. Therefore, in order to proceed further in our investigation, and for the sake of convenience and consistency, it appears that by substituting Eqs. (18) - (21) and within the framework of the relationship given by Eq. (16), Eq. (17) can be given according to δ and reduce to:

$$r^2\delta^{\frac{p+2r}{r}}\Phi_{\delta\delta}+\Gamma_3 a_0^2\delta^{\frac{3p}{r}}\Phi^3=0, \tag{22}$$

which cannot be solved as a differential equation unless the powers of δ are equal, leading to the condition

$$p+2r=3p. \tag{23}$$

In this case, as seen, Eq. (22) turns into a differential equation with variable coefficients, the solution of which is only possible for $p+2r=3p$, leading to the following constraint relative to the dynamics of the tubulin systems

$$p=r\neq 0. \tag{24}$$

Accordingly, we can firstly re-express Eq. (22) as:

$$r^2\Phi_{\delta\delta}+\Gamma_3 a_0^2\Phi^3=0. \tag{25}$$

Next, by using the condition given by Eq. (24) and without loss of generality, Eq. (21) conveniently provide $p=r=1/3$. So, Eq. (25) can be finally transformed in the following form:

$$\Phi_{\delta\delta}+9\Gamma_3 a_0^2\Phi^3=0. \tag{26}$$

In addition, by setting $a_0^2=-\frac{2}{9\Gamma_3}$, Eq. (26) can now be transformed into a simplified ODE of the form:

$$\Phi_{\delta\delta}-2\Phi^3=0. \tag{27}$$

Accordingly, by multiplying Eq. (18) by 3, and then using Eq. (20), the relations of Eqs. (18) and (19) yield after making appropriate transformations to the following two equations:

$$2\Gamma_2\eta_0^2+3\Gamma_1\eta_0+3\Gamma_0=0, \tag{28}$$

$$\Gamma_2\eta_0+\Gamma_1+\frac{2}{9}=0,. \tag{29}$$

Furthermore, from Eqs. (29) and by using the expressions of Γ_1, Γ_2 and Γ_3 given in Eq. (14), we can easily derive a convenient expression for α explicitly expressed as:

$$\alpha=\frac{\rho}{2\beta\eta_0}\left[-1\pm\sqrt{1-\frac{8\beta\rho\eta_0}{9}}\right],\qquad \beta\rho\eta_0\leq 9/8. \tag{30}$$

It is noteworthy that, Eq. (30) suggests that α can be negative or positive. Accordingly, at this level and again without loss of generality, in the rest of the analysis we will consider η_0 arbitrary (constant) in order to derive non diverging solutions.

More precisely, it is important to notice here that in other to have existing solutions, the minus (-) sign in the expression of a_0 must disappear, such that a_0 will be positive. Proceeding further into our investigation, let us multiply both sides of Eq. (27) by Φ_δ, and performing a direct integration brings about a fundamental ordinary differential equation given by:

$$\Phi_\delta^2=\Phi^4+\Phi_0, \tag{31}$$

where Φ_0 is an arbitrary constant of integration. This is a crucial equation whose solution will be used to explain the nonlinear dynamics of MTs. As far as Eq. (31) is concerned, the divergence of the solution Φ can only be prevented by finding the exact solution to Eq. (31) in function of z. In this regards, we can derive corresponding expressions for the functions ξ, δ and η. Alternatively, by considering Eqs. (10) and (12), and by making use of the relation $\eta=\mu_0\psi$, we can finally obtain the following relations:

$$\eta_\xi=\frac{1}{\xi\phi(\eta)}=\mu_0\psi_\xi, \tag{32}$$

$$\phi(\eta)=\frac{1}{\psi_z}. \tag{33}$$

Now substituting $\phi(\eta)$ from the expression in the right hand side of the first equality in Eq. (32), and by equating it with Eq. (33), we obtain the equation $\mu_0\xi\frac{\partial\psi}{\partial\xi}=\frac{\partial\psi}{\partial z}$. Furthermore, by solving the resultant set of equations recursively, and with the aid of definitions Eq. (16), we can obtain the explicit expressions for the pertaining functions ξ and δ. After some algebra we therefore get the expressions for the functions ξ and δ respectively as:

$$\xi(z)=\xi_0\exp(\mu_0 z), \tag{34}$$

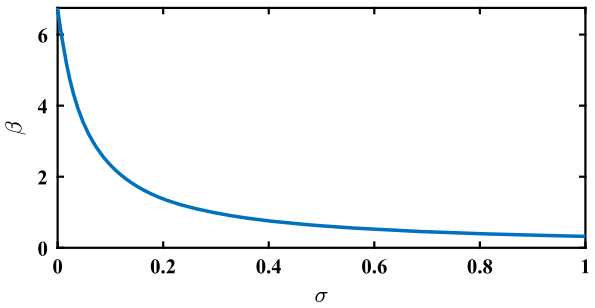

Fig. 2. Evolution of the parameter β as a function of σ. The other dimensionless parameters are chosen as $\rho = 0.5$ and $\eta_0 = -1.0$.

and

$$\delta(z) = \xi_0 \exp(\frac{1}{3}\mu_0\, z). \tag{35}$$

It is obvious that both functions ξ and δ, which are now determined as a function of the unified variable z, have almost the same form and are almost equal for small $|\mu_0|$, indicating that both functions have equal physical meaning. This is very interesting result indicating again the appropriateness of the transformation Eq. (15). Here it noteworthy that its physical explanation is simple as both functions describe ξ and δ describe same physics.

In the rest of this investigation and without loss of generality, let us set for simplicity $\xi_0 = 1$. Finally, the solution of Eq. (31) is obtained by substituting Eqs. (34) and (35) into the said solution, and hence different solutions can be derived depending on the conditions on Φ_0. From Eq. (16), the general explicit form of the function $\eta(z)$ can be obtained as:

$$\begin{aligned}\eta(z) &= \sqrt{-\frac{2}{9\Gamma_3}}\exp(\frac{1}{3}\mu_0\, z)\,\varphi(z) + \frac{\Gamma_2}{3\Gamma_3} \\ &= \sqrt{\frac{-2\rho^4}{9\alpha^3}}\exp(\frac{1}{3}\mu_0\, z)\,\varphi(z) + \eta_0,\end{aligned} \tag{36}$$

provided the expression of the continuous function $\varphi(z) = \Phi(\delta)$ should be known. In the same vein, by using Eqs. (34), (35) and (36), as well as the relation $\eta = \mu_0\psi$, and after some algebra while making appropriate scaling and transformations, and with the aid of the definitions Eq. (31), we can write down the explicit expression of the function $\psi(z)$ in terms of original model parameters as:

$$\begin{aligned}\psi(z) &= \frac{\alpha}{\rho}\left[\sqrt{-\frac{2}{9\Gamma_3}}\exp(\frac{\rho}{3\alpha}\, z)\,\varphi(z) + \frac{\Gamma_2}{3\Gamma_3}\right] \\ &= \frac{\alpha}{\rho}\left[\sqrt{\frac{-2\rho^4}{9\alpha^3}}\exp(\frac{\rho}{3\alpha}\, z)\,\varphi(z) + \eta_0\right].\end{aligned} \tag{37}$$

More evidently, Eq. (37) shows that the derived solutions depend explicitly on α, ρ and η_0, which remain the single mathematical parameters that significantly simplify the estimations of expressions of the solutions $\psi(z)$.

On the other hand, there is no experimental values for some model parameters or no way to determine their exact values, and the best we can do is to follow some requirements and deduce possible intervals for the said parameters, resulting to a plausible better choice and estimation, and hence for the discussion of the nature of evolution of solutions under each case. From a physical point of view, the study of propagation of nonlinear waves in MTs is an exciting and important task. In this regards, by using Eq. (28), as well as the expression of α given in Eq. (30), we can straightforwardly obtain the following plausible two expressions of β as:

$$\beta = \frac{27(9\sigma - 2\rho\eta_0)}{(27\sigma - 4\rho\eta_0)^2}. \tag{38}$$

Accordingly, we can set the expression of η_0 given in Eq. (20) to be its general expression because this expression of η_0 allows an explicit relation between the parameters of the system as expressed in Eq. (28) and Eq. (29). In this regards, we consider Eqs. (28) and (29) to yield the same expression for η_0, since it is an arbitrary constant.

From Eq. (38), and the important considerations and definitions from Eq. (7), it appears that $\sigma > \frac{2\rho\eta_0}{9}$, leading to $\beta > 0$.

Fig. 2 presents the evolution of the model parameter β as a function of the parameter σ as given by Eqs. (38) and for fixed values of ρ and η_0. Indeed, in accordance with the hypotheses and physical requirements, we have selected the parameters as $\rho = 0.5$ and $\eta_0 = -1.0$, and which insure that $\alpha < 0$. Thus, using the appropriate relation between Γ_3, Γ_0, Γ_1 and Γ_2 obtained from Eqs. (20) and (28), will lead to the condition $a_0^2 > 0$, which is in accordance with the hypotheses and physical requirements. From this figure, it can be seen that as the linear part of the additional potential energy $V_2(u_n)$ through the uniform intrinsic electric field strength and defined above as V_{el} (as in Fig. 1) is important, the nonlinear one decreases monotonically (abruptly and then smoothly) and progressively

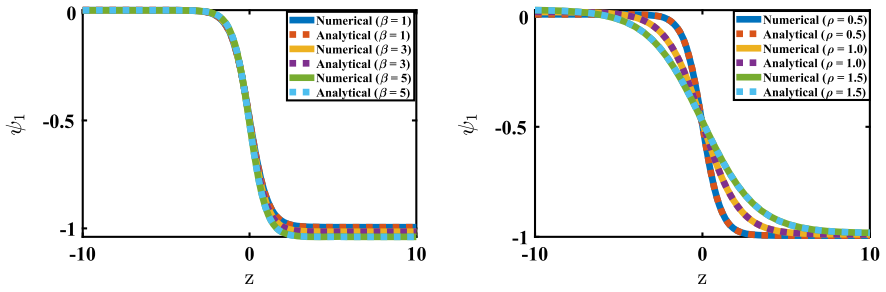

Fig. 3. Wave form of traveling anti-kink soliton solution in the stationary state, plotted analytically (solid lines) and numerically (dotted lines) for $\eta_0 = -1.0$, and (a) different values of β and (b) different values of ρ, respectively. For the left figure (a) $\rho = 0.5$ and $\beta = 1.0$ (blue and red colors), 3.0 (yellow and purple colors) and 5.0 (cyan and green colors), respectively; while for the right figure (b) $\beta = 1.0$ and $\rho = 0.5$ (blue and red colors), 1.0 (yellow and purple colors) and 1.5 (cyan and green colors), respectively.

becomes of the order of zero as σ increases, indicating the saturation behavior of the parameter β as σ increases. Moreover, the graph suggests that when the linear part of the additional potential energy $V_2(u_n)$ due the intrinsic electric field strength is very small, the nonlinear part should be very strong to in order to compensate. The important aspect of this result is that the interplay between parameters β, σ and ρ is crucial for the stability of the obtained solutions. Among other things, also from Fig. 2, it can be seen from the evolution of the σ dependence of the parameter β that the oscillations of tubulin dimers are a cooperative phenomenon, governed not only by the predominant variation of the polarized cytoplasmic water and motor proteins (enzymes), but also by many other properties. Another important point is that, regarding the expression of α given in Eq. (30), and considering the important condition $\beta > 0$ from Eq. (38), we conclude that $\alpha < 0$.

3. Results and discussions

As generally known, solving Eq. (31) can provide a richness of wave solutions depending on the mathematical tools explored. A part of the difficulty stems from the fact that resolution of such equation requires specific considerations or conditions which involve various technical difficulties coming from the fact that Eq. (31) is an ODE. Then, the possible solutions of Eq. (6) can be obtained in terms of exponential functions, Jacobi elliptic and Weierstrass $\wp$ functions [54,55,65–69].

In this regards, in order to overcome the technical difficulty, we shall not be so much concerned with technical details and all the tedious derivations. Instead, two sets of solutions are considered, depending on the condition on the arbitrary constant of integration Φ_0, i.e., $\Phi_0 = 0$ and $\Phi_0 \neq 0$, respectively. Moreover, Eq. (6) is analytically addressed using mathematical methods mentioned above with a couple of conditions, and completely different solutions have been derived. Therefore, in what follows and in order to proceed further, we will investigate and analyze the obtained solutions and perform numerical analysis using the standard fourth-order Runge–Kutta scheme, followed by a numerical simulation of their time evolution, taking into account the expression of α given by Eq. (30), as well as different values of β obtained from Fig. 2.

Now setting $\Phi_0 = 0$, and after appropriate calculations, one can write down the explicit form of one soliton solutions in terms of exponential function as [67–69]:

$$\psi_1(z) = \frac{\alpha}{\rho}\left[-\frac{\sqrt{\frac{-2\rho^4}{9\alpha^3}}\exp\left(\frac{\rho}{3\alpha}z\right)}{\exp\left(\frac{\rho}{3\alpha}z\right)+z_0}+\eta_0\right]. \tag{39}$$

Likewise, setting $z_0 = \pm 1$ yields, and after appropriated calculations, two different final expressions of the solution given by Eq. (39) which are reminiscent to tanh- and coth-functions [27,34,69,80]. However, only one solution is physically acceptable for our problem, i.e., for $z_0 = 1$ and which can finally be expressed as:

$$\psi_1(z) = \frac{\alpha}{\rho}\left\{\sqrt{\frac{-2\rho^4}{9\alpha^3}}\left[\frac{1}{2}-\frac{1}{2}\tanh\left(\frac{\rho}{6\alpha}z\right)\right]+\eta_0\right\}. \tag{40}$$

Fig. 3 presents the stationary evolution of function ψ as a localized anti-kink soliton solution (anti-kinkon) of the ODE given by Eq. (6) for different values of the parameters ρ (different strengths of the viscous effect) and β (different strengths of the polyelectrolyte effect) or σ (different strengths of the linear electric field effect), respectively.

Accordingly, Fig. 3 displays the evolution of the solution ψ_1 predicted by Eq. (40) as a function of the unified variable z, in the form of localized anti-kink soliton, for different values of parameters β, ρ and a fixed value of η_0 ($\eta_0 = -1.0$). Following the anti-kink profiles, Fig. 3 shows that depending on the values of the parameters β and ρ, the anti-kinkon solution profiles manifest amplitude and waveform or width variations, this depending on the values of the parameters β and ρ. As shown in Figs. 3(a) and (b), it appears clearly that the amplitude and width of anti-kink-type soliton solution increases and decreases with increasing and decreasing β and ρ, respectively, leading to the important influence of the damping and polyelectrolyte effects. In this respect, it is obvious that the

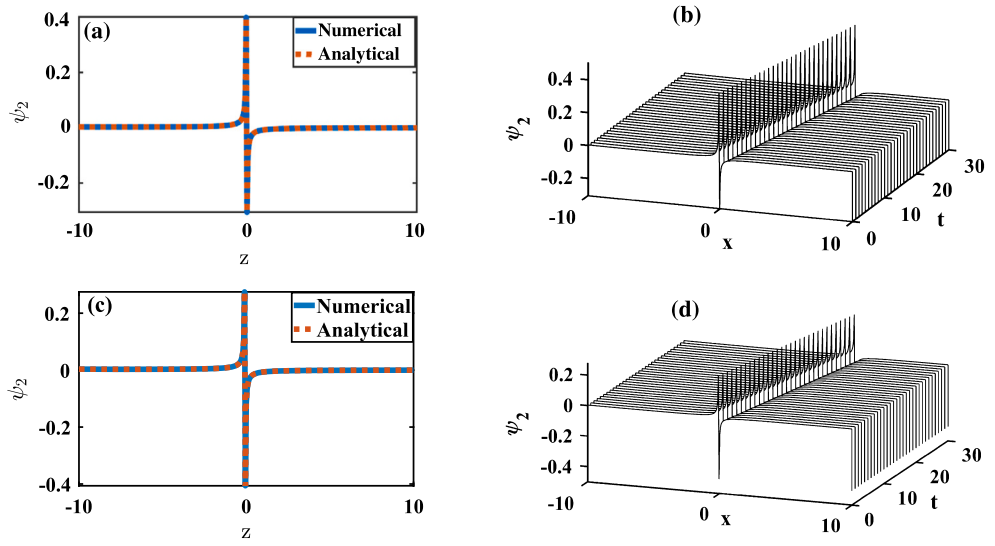

Fig. 4. Numerical (solid lines) and analytical (dotted lines) generations of localized discrete soliton-like modes (left figures) and their propagation (right figures) in the MTs showing the effects of the model parameters for η_0 = -1.0, ρ = 0.5, κ = 0.7; and: (a) and (b) β = 1.0, (c) and (d) β = 3.0.

amplitude and the waveform of the anti-kink-like excitation or soliton increases and changes with increasing β, as clearly seen in Fig. 3(a) where β = 1.0 (blue and red), 3.0 (yellow and purple) and 5.0 (cyan and green) colors, respectively. On the other hand, the damping effects on the anti-kinkon's amplitude and profiles or width are highlighted when increasing ρ, as shown in Fig. 3(b) for β = 1.0, ρ = 0.5 (blue and red colors), 1.0 (yellow and purple colors) and 1.5 (blue and green colors), respectively. More specifically, all these findings suggest that a further increase in β or decrease in ρ may lead to a more steepened ramp in the anti-kink soliton and the higher end of the anti-kinkon heightens more and more with the increased amplitude, which may give a different picture of understanding the peculiar dynamical effect known as "treadmilling", in MTs.

Among other things, it appears that the parameter β is an important factor in the rapid propagation of solitonic waves and in the very interesting assembly and disassembly behavior in MTs, as can be seen in Fig. 3(a). Therefore, all these aspects noticed and illustrated in Fig. 3, sufficiently demonstrate that in addition to kink-like domain walls, anti-kink-like dynamics can be viewed as bits of information propagating along the MTs [12,27]. This form of dynamics or transport governed by anti-kink-type soliton solutions is known as anterograde mechanism for the movement of motor proteins [13,81–83].

On the other hand, by considering the constant of integration $\Phi_0 \neq 0$, a careful integration of Eq. (31) can lead to a solution ψ in terms of Jacobi elliptic function [54,55,65–67], *viz*

$$\psi_2(z) = \frac{\alpha}{\rho}\left[\sqrt{\frac{-2\rho^4}{9\alpha^3}}\exp\left(\frac{\rho}{3\alpha}z\right)\frac{1}{\sqrt{2}\,\mathrm{cn}[\exp\left(\frac{\rho}{3\alpha}z\right),\kappa]} + \eta_0\right], \tag{41}$$

where cn is the Jacobi elliptic function with modulus κ ($0 < \kappa \leq 1$), and which is obtained to be equal to 0.7 here. Quite remarquably here, the quantity κ turns out to be a non arbitrary constant, i.e., fixed. In fact it depends on the defined parameters of the model [29,54,55]. Before continuing, we would like to make a few more additional observations or additional remarks on the solution that was derived above using Eq. (41). Of course, it should be noted that, for the sake of simplicity, we are considering the integration constant Φ_0 to be undeniably negative, i.e., we choose $\Phi_0 = -1$, and the Jacobi elliptic function cn representing standard Jacobian elliptic function with modulus κ [54,55,67].

Figs. 4 and 5 display the analytical (dots) and numerical (solid lines) localized patterns of discrete modes as function of the unified variable z, and their evolution in the $x-t$ plane for two different values of β and two different values of ρ, while η_0 = -1.0. Accordingly, the discrete modes are spatially localized and their lifetime depends on the cooperative interactions between the parameters β and ρ as can be seen in Figs. 4 and 5. More precisely, the 2-D representation of these discrete modes (left graphs) and their propagation with time (right graphs) for different values of parameters β and ρ show that the initial localized discrete patterns persist as time evolves, illustrating the fact that the behavior of the localized discrete modes in MTs is acceptable as the soliton, as depicted in Figs. 4(a)-(d) and Fig. 5(a)-(d). Additionally, the study offers compelling proof of the influence of the parameter β on the behavior of discrete patterns through the mode profiles, showing that the amplitudes of the discrete modes seem not altered as the waves are propagating, demonstrating the stability of the localized discrete modes, as shown in Figs. 4(b) and 4(d), and Figs. 5(b) and 5(d). Among other things, from the results it is evident that recurrence is observed as time passes and such discrete modes are intrinsically generated as a response to the combined effects of nonlinearity and spatial discreteness [84]. However, from the solution given by Eq. (41), these localized discrete modes are generated in complex cooperative interaction incorporating ferroelectric processes, dispersion, dissipation, discreteness and nonlinearity, and it appears that these modes are structurally and symmetrically non uniform, since

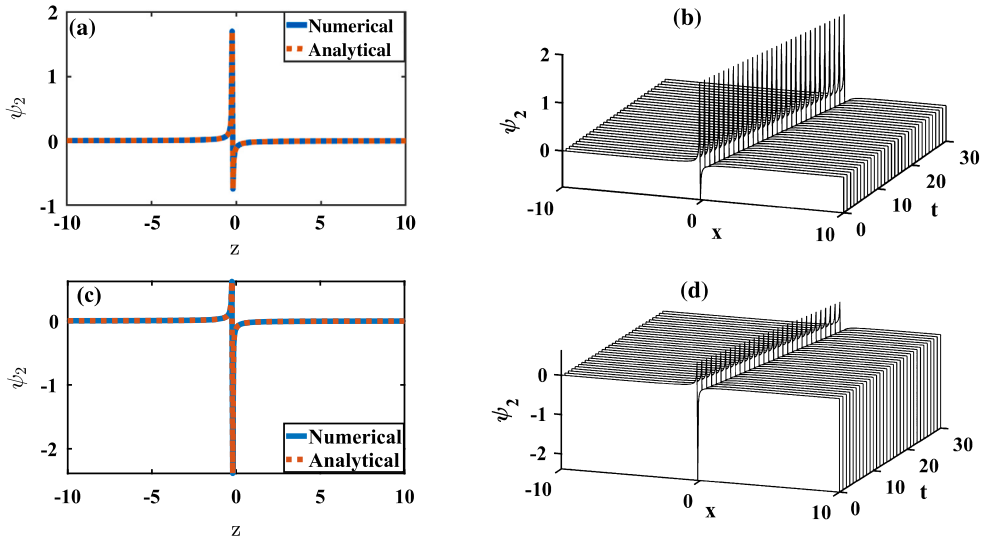

Fig. 5. Numerical (solid lines) and analytical (dotted lines) generations of localized discrete soliton-like modes (left figures) and their propagation (right figures) in the MTs showing the effects of the model parameters for η_0 = -1.0, ρ = 1.5, κ = 0.7, and: (a) and (b) β = 1.0; (c) and (d) β = 3.0.

their spatial profile and symmetry alter with β and ρ during their process of development, as they propagate through the tubulin $\alpha\beta$-heterodimers lattice.

Most interestingly, taking the initial value of β in the analysis to be β = 1.0, it is shown that a slight variation of its value, i.e., for example by considering β = 3.0, has a direct incidence on the modes symmetries and on their amplitudes, as can be seen in Figs. 4(a) and 4(c) and Figs. 5(a) and 5(c), respectively. On the order hand, it is noteworthy that we are looking for all possible solutions based on constraints and assumptions. Indeed Eq. (6) can be solved from another perspective, following the method, the procedures and steps developed, presented and explained in Refs. [65,66,68], and to which the reader is referred for more details. Accordingly, by using Eqs. (6) and (31), and solving the set of equations following the same procedure and steps, yielding to another general solution of ψ expressed in terms of Weierstrass $\wp$-function [68,69,79]. Proceeding with our investigation and assumption, a general solution ψ is derived and expressed as:

$$\psi_3(z) = \frac{\alpha}{\rho}\left[\sqrt{\frac{-2\rho^4}{9\alpha^3}}\,\delta\,\frac{\wp'(\delta, g_2, 0)}{\wp(\delta, g_2, 0)} + \eta_0\right], \tag{42}$$

where $g_2 \equiv \Phi_0$ is a free parameter, and δ is defined in Eq. (35). Meanwhile, the Weierstrass $\wp$-function can be associated to Jacobi elliptic function considering different values of g_2. Here, it might be interesting to point out that the case where g_2 = 0 has been already analyzed as it is equivalent to the case where Φ_0 = 0, given by solution ψ_1. However, when $g_2 < 0$, the Weierstrass $\wp$-function can expressed as follows [54,68,69]:

$$\wp(\delta) = \nu_0 + 2\,\nu_0 \mathrm{sn}^{-2}(\sqrt{2\,\nu_0}\,\delta, \kappa), \tag{43}$$

where obviously κ is the modulus of the Jacobi elliptic function sn, with $0 < \kappa \leq 1$, and ν_0 is an appropriate fundamental function of g_2.

In Fig. 6, we display in this case the profile of the associated solitonic solution obtained both analytically and numerically using $\psi_3(z)$ and the solution in Eq. (43) as a function of the unified variable z, and achieve its evolution (propagation) in the $x-t$ plane for chosen values of model parameters defined above, i.e., η_0 = -1.0, ρ = 0.5, β = 1.0, κ = 1, and ν_0 = 0.3. Here, we observe that the solution is a space-localized pattern with perfect soliton-like profile emerging as an asymmetric dark solitary-wave, as depicted in Fig. 6(a). Also, its evolution in the $x-t$ plane suggests the persistence of the initial dark soliton pattern as time evolves, which demonstrates the stability of the asymmetric dark-type soliton solution, as can be seen in Fig. 6(b).

Following the same procedure as above, when $g_2 > 0$, the explicit form of the Weierstrass $\wp$-function in this case can be written down as [54,68,69]:

$$\wp(\delta) = \upsilon_0\left[1 - \mathrm{cn}^2(\sqrt{\upsilon_0}\,\delta, \kappa)\right], \tag{44}$$

where cn is a well-known Jacobi elliptic function with modulus κ introduced above and δ is the function defined in Eq. (35), whereas υ_0 is another appropriate fundamental function of g_2. Fig. 7 presents the profile of the associated soliton-like solution obtained numerically using the solution given by Eq. (44) as function of the unified variable z, and its propagation in the $x-t$ plane for the same chosen values of the model parameters taken above, i.e., η_0 = -1.0, ρ = 0.5, β = 1.0, κ = 1, and υ_0 = 1.0. Accordingly, for the same chosen values of the model parameters, it appears that the solution is also a space-localized pattern of soliton-like

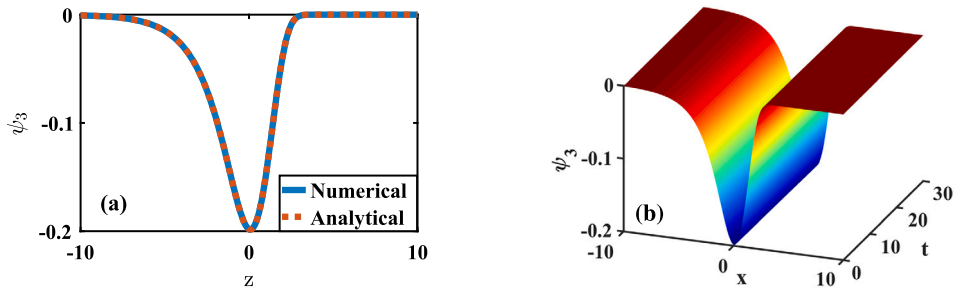

Fig. 6. Numerical (solid line) and analytical (dotted line) generation of a localized asymmetric dark soliton profile in MTs system, solution of Eq. (6) as function of the unified variable z (a), and its evolution in the $x-t$ plane (b), for $\eta_0 = 1.0$, $\rho = 0.5$, $\beta = 1.0$, $\kappa = 1$ and $v_0 = 0.3$. The analytical solution is given by $\psi_3(z)$ [Eq. (42) and Eq. (43)].

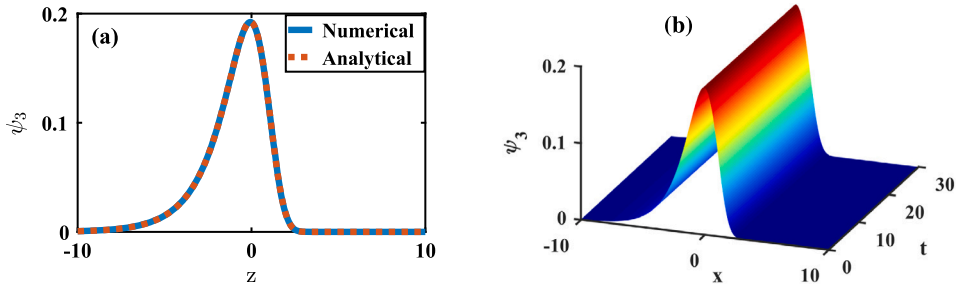

Fig. 7. Numerical (solid line) and analytical (dotted line) generation of a localized asymmetrical bright-type soliton profile in MTs system, solution of Eq. (6), as function of the unified variable z (a) and its evolution in the $x-t$ plane (b) for $\eta_0 = -1.0$, $\rho = 0.5$, $\beta = 1.0$, $\kappa = 1$ and $v_0 = 1.0$. The analytical solution is given by $\psi_3(z)$ [Eqs. (42) and (44)].

profile emerging as an asymmetric bright soliton, as presented in Fig. 7(a). Here again, the propagation in the $x-t$ plane leads to a stable solution, as can be clearly seen in Fig. 7(b). From Figs. 6(b) and 7(b), it can be seen from the propagation of the soliton-like modes or excitations that the amplitude and the width of the dark and bright soliton profiles do not vary as time evolves, which is characteristic of the stability of the soliton-like solutions. According to the parameters of MT dimers, and based on the initial condition, it is apparent that localized discrete and soliton-like modes are accessible as nonlinear dynamical behaviors in MTs, provided that the model parameters are fine tuned. It is worth mentioning that Figs. 6 and 7 show the behavior of bright and dark soliton-like modes depending on the sign of the free parameter g_2. Among other things, stable pulse-type solitons are obtained (emerge and propagate) depending on the values of the parameters σ, β and ρ.

Moreover, we have performed an analytical analysis of Eq. (6) using the solutions obtained and the numerical analysis using the Runge Kutta 4 scheme, followed by a numerical simulation of their time evolution, taking into account the expression of α given by Eq. (30), and we observe a good agreement between analytical and numerical analysis of the localized stationary solutions.

More interestingly, all these various features underlying the nonlinear dynamics of MTs can be relevant to many biological processes such as chemical energy transition in the process of hydrolysis of GTP nucleotides and microtubule motor proteins transport such as kinesins and dyneins [13,82,83], cell growth and division for which MTs disassemble and reassemble [6,12,78,85], excitations and inhibition of biomembranes and neurons [6,14,86], intracellular transport and transport of both proteins and organelles [21, 30,87], cellular movements including separating chromosomes during mitosis and meiosis [20,88], transport of cellular cargo [89], respiratory infections [90], dynamic information processing including processing, propagation, storage and transduction, of biological information in MTs [2,6,14,15,17–19]. Among other things and of capital importance, it appears that all the solution obtained assume forms or profiles of more stables and robust solitons.

As explained above, the solutions obtained can be divided on several types. Kink-like solutions, i.e., antikink-type soliton solutions coincide with those obtained by other methods, like tanh-expansion and simplest equation methods [25–28,38–42], and which can be viewed as bits of information propagating along MTs [11–15,34]. For example such kink-like solutions may be involved in the movement of motor proteins, in agreement with the treatment of MTs as artificial information strings and demonstrating that filamentary cytoskeletal structures may operate much like information strings in analogy to semiconductor word processors [2, 6,8–14]. On the other hand, new classes of asymmetric bell-shape soliton solutions (asymmetric dark-bright soliton-like modes) and discrete modes in terms of special functions are also obtained in comparison with the symmetric bell-type solitons previously obtained [27]. Although, these solutions are new and previously have not been described in previous works, they demonstrate that pulse-type solitons can propagate along MTs owing to the coupling between the elastic states of the tubulin dimers and are produced, for instance, by the energy released during GTP hydrolysis [27,91].

4. Stability analysis

Among other things and as widely known, it is always very important to investigate the stability of all the solutions that are produced, which is the goal of this section. Accordingly, let us examine the stability of the solutions derived previously. In this order of idea, and considering the analysis method proposed in [76], we will focus on the unified solution given by Eq. (37). Thus, in order to investigate the stability of our solutions, let us begin by expressing the function ψ as follows:

$$\psi = \psi_s + \psi_p, \tag{45}$$

where ψ_s corresponds to ψ_1, ψ_2 and ψ_3, while ψ_p is a small perturbation. Therefore, introducing Eq. (45) into Eqs. (6), and linearizing with respect to ψ_p yields the following second order differential equation:

$$\psi_p'' - \frac{\rho}{\alpha}\psi_p' + \frac{3}{\alpha}\psi_s^2\psi_p - \frac{2\beta}{\alpha}\psi_s\psi_p - \frac{1}{\alpha}\psi_p = 0. \tag{46}$$

Furthermore, assuming that $\psi_p' = \Lambda$ and linearizing the product $\psi_s^n\psi_p$ $(n = 1, 2)$, we can obtain a system of linearized ODEs [76], which is

$$\begin{cases} \psi_p' = \Lambda, \\ \Lambda' = \frac{\rho}{\alpha}\Lambda - \frac{3\alpha^2\eta_0^2 - 2\beta\alpha\eta_0 - \rho}{\rho\alpha}\psi_p. \end{cases} \tag{47}$$

In addition, it is convenient to express the system in Eq. (47) in the matrix form as:

$$\begin{bmatrix} \psi_p' \\ \Lambda' \end{bmatrix} = \begin{bmatrix} 0 & 1 \\ -\frac{3\alpha^2\eta_0^2 - 2\beta\alpha\eta_0 - \rho}{\rho\alpha} & \frac{\rho}{\alpha} \end{bmatrix} \begin{bmatrix} \psi_p \\ \Lambda \end{bmatrix}. \tag{48}$$

Setting $A^* = \begin{bmatrix} 0 & 1 \\ -\frac{3\alpha^2\eta_0^2 - 2\beta\alpha\eta_0 - \rho}{\rho\alpha} & \frac{\rho}{\alpha} \end{bmatrix}$ and $V^* = \begin{bmatrix} \psi_p \\ \Gamma \end{bmatrix}$, transforms Eq. (48) can be transformed into an eigenvalue problem of the form:

$$T(\lambda) = \det(A^* - \lambda I) = 0, \tag{49}$$

where λ is the eigenvalue and I is the identity matrix. Hence, by solving the eigenvalue problem given by Eq. (49) brings about a quadratic characteristic equation given as:

$$\lambda^2 - \frac{\rho}{\alpha}\lambda + \frac{3\alpha^2\eta_0^2 - 2\beta\alpha\eta_0 - \rho}{\rho\alpha} = 0. \tag{50}$$

Consequently, after some simple mathematical algebra, the solutions of the characteristic equation can be obtained and expressed as:

$$\lambda_{1,2} = \frac{\rho}{\alpha}\left[\frac{1 \pm \sqrt{1 - \frac{4\alpha(3\alpha^2\eta_0^2 - 2\beta\alpha\eta_0 - \rho)}{\rho^3}}}{2}\right], \tag{51}$$

where the subscripts 1 and 2 refer to the plus and minus signs respectively. Accordingly, the growth rate of the disturbances represented by the real part of the eigenvalue λ, $[\mathrm{Re}(\lambda)]$ is a determining factor for understanding the stability of our solutions. In this regards, the solutions are stable if $\mathrm{Re}(\lambda) < 0$. According to the expression in Eq. (51), we can notice that first of all λ_s are real, and secondly λ_s can take positive as well as negative values. On the other hand, the expression of α is positive, this implies that the solutions derived are stable whenever $\lambda < 0$. Therefore, following the above analytical stability analysis of the obtained solutions, it is evident that the stability of the soliton-like solutions seems to be achieved due to the balance between the nonlinearities and the dissipation.

5. Conclusion

In the present study and to gain a better understanding of microtubule dynamics, we developed a modified u-mode for MTs that considers the polyectrolyte properties of the tubulin molecules. In this regards, we have introduced a cubic nonlinear term in the electric field potential of the u-model, that account for the nonlinear electric interactions in the MTs resulting from the combined effects of the intrinsic electric field, the polarized cytoplasmic water and enzymes surrounding the MTs. Therefore, to study the nonlinear dynamics of MTs, the corresponding dynamical equation governing the dynamics of tubulin systems is obtained, and a modified mathematical approach proposed by Samsonov [65] is used to find the solitary wave solutions of the relevant modes describing the dynamics of the microtubulin system. The results of our investigation have shown that the localized waves or excitations responsible for energy transfer within tubulin dimers, and which further are of capital importance for the mechanisms of assembly

and disassembly in MTs, can evolve either as localized kink-like solitons (antikink-type soliton solutions), discrete soliton-like modes, asymmetric bright-solitons or asymmetric dark-type solitons. These soliton-like solutions arise from the requirement that β is positive, such that α will be negative. The condition on α means that the kenetic energy of the dimers is not predominant in its competitive interactions with the chemical bounds.

In spite of nonlinearities in microtubulin systems, the nonlinear dynamics of MTs is found to be governed by stable localized antikink-like excitations, discrete soliton-like modes and asymmetry dark- and bright-type soliton solutions, demonstrating the complex nonlinear dynamics of the microtubulin systems. Also, it is interesting that the description of the nonlinear dynamics of MTs depend on applied mathematical procedures. Therefore, we investigate the solitary wave solutions of the proposed MTs model using the above proposed mathematical method. We guesswork that the existence of such nonlinear dynamics or quanta of energy transfer in the form of discrete patterns and solitonic waves would provide a new understanding of the motor protein transport mechanism on the stability of MTs in various cellular activities such as growth and division in microtubulin systems, and which are crucial for living state. In fact, it has been shown experimentally that tubulin dimer is subjected to a conformational change due to the hydrolysis of GTP into GDP and binding, in which one tubulin monomer (α or β) deviates its orientation from the vertical axis of the dimers, resulting in the motion of the kinesin along MTs [17]. The finding of such localized discrete, asymmetric dark- and bright-solitons-like modes in MTs seems to lay down a milestone for a better understanding of the biological functions of MTs and cytoskeletal structures, which primarily dependent on their mechanical properties, as well as some specific myocardial cell functions in which MTs are involved, including regulation of contraction, ion channel function, receptor recycling, and sarcomere structure [34,70,72,92]. The investigation of nonlinear wave propagation in microtubules is an intriguing and significant task from a physics perspective. In order to show that the obtained soliton-like solutions assume a form of more stable and robust solitons, we next investigate the propagation of the obtained nonlinear solitary waves in the microtubulin systems. This is relevant to a variety of biological processes, including the energy transition of GTP hydrolysis, cell growth, excitation and inhibition of neurons, and so forth. However, it is crucial to note that the model presented in this study is a mechanical one, although there have been attempts to portray MT as a nonlinear electrical transmission line [30–33]. Consequently, a combination model, that is, an electro-mechanical model for electro-mechanical excitations in the microtubulin system, will be particularly significant [9,88,90]. Likewise, it should be noted that every solution examined in this study is a one-soliton solution. Accordingly, investigating potential multisoliton solutions for the microtubulin systems should therefore be one of the upcoming research.

CRediT authorship contribution statement

Remi Jean Noumana Issokolo: Writing – review & editing, Writing – original draft, Validation, Software, Methodology, Investigation, Formal analysis, Conceptualization. **Serges Eric Mkam Tchouobiap:** Writing – review & editing, Writing – original draft, Validation, Supervision, Software, Resources, Methodology, Investigation, Formal analysis, Conceptualization. **Fernand Naha Nzoupe:** Writing – review & editing, Writing – original draft, Validation, Software, Methodology, Investigation, Formal analysis.

Ethics approval and consent to participate

Not applicable.

Additional information

No additional information is available for this paper.

Declaration of competing interest

The authors declare that they have no known competing financial interests or personal relationships that could have appeared to influence the work reported in this paper.

Acknowledgements

One of the authors MTSE gratefully acknowledges the support from The World Academy of Sciences (TWAS), Trieste, Italy, within the framework of the TWAS-UNESCO Associateship Scheme - Ref. 3240290072 - with iThemba LABS-National Research Foundation, Somersest, West, South Africa.

Data availability

No data was used for the research described in the article.

References

[1] H. Lodish, A. Berk, P. Matsudaira, C.A. Kaiser, M. Krieger, M.P. Scott, L. Zipursky, J. Darnell, Molecular Cell Biology, fifth ed., W. H. Freeman, New York, 2008, https://pdfcoffee.com/molecular-cell-biology-lodish-5th-ed-pdf-free.html.

[2] P. Dustin, Microtubules, 2nd revised ed., Springer-Berlin, Heidelberg, 1984.
[3] M.J. Levitt, Computer simulation of DNA double-helix dynamics, Cold Spring Harbor Symp. Quant. Biol. 47 (1983) 251, https://doi.org/10.1101/sqb.1983.047.01.030.
[4] J.A. Tuszyński, J.A. Brown, E. Crawford, E.J. Carpenter, M.L.A. Nip, J.M. Dixon, M.V. Satarić, Molecular dynamics simulations of tubulin structure and calculations of electrostatic properties of microtubules, Math. Comput. Model. 41 (2005) 1055, https://doi.org/10.1016/j.mcm.2005.05.002.
[5] J.A. Tuszyński, S. Hameroff, M.V. Satarić, B. Trpisová, M.L.A. Nip, Ferroelectric behavior in microtubule dipole lattices: implications for information processing, signaling and assembly/disassembly, J. Theor. Biol. 174 (1995) 371, https://doi.org/10.1006/jtbi.1995.0105.
[6] S. Hameroff, R. Penrose, Consciousness in the universe: a review of the 'Orch 0R' theory, Phys. Life Rev. 11 (2014) 39, https://doi.org/10.1016/j.plrev.2013.08.002.
[7] M.V. Satarić, R.B. Žakula, J.A. Tuszyński, A model of the energy transfer mechanism in microtubules involving a single soliton, Nanobiology 1 (1992) 445, http://refhub.elsevier.com/S0096-3003(14)00484-6/h0015.
[8] M. Cifra, J. Pokorný, D. Havelka, O. Kučera, Electric field generated by axial longitudinal vibration modes of microtubule, Biosystems 100 (2010) 122, https://doi.org/10.1016/j.biosystems.2010.02.007.
[9] O. Kučera, D. Havelka, Mechano-electrical vibrations of microtubules-link to subcellular morphology, Biosystems 109 (2012) 346, https://doi.org/10.1016/j.biosystems.2012.04.009.
[10] J. Tabony, D. Job, Gravitational symmetry breaking in microtubular dissipative structures, Proc. Natl. Acad. Sci. USA 89 (15) (1992) 6948, https://doi.org/10.1073/pnas.89.15.6948.
[11] S. Zdravković, Microtubules: a network for solitary waves, J. Serb. Chem. Soc. 82 (2017) 1, https://doi.org/10.2298/JSC161118020Z.
[12] M.V. Satarić, J.A. Tuszynski, R.B. Žakula, Kinklike excitations as an energy-transfer mechanism in microtubules, Phys. Rev. E 48 (1993) 589–597, https://doi.org/10.1103/PhysRevE.48.589.
[13] B. Mickey, J. Howard, Rigidity of microtubules is increased by stabilizing agents, J. Cell Biol. 130 (1995) 909, https://doi.org/10.1083/jcb.130.4.909.
[14] S.R. Hameroff, R.C. Watt, Information processing in microtubules, J. Theor. Biol. 98 (1982) 549, https://doi.org/10.1016/0022-5193(82)90137-0.
[15] T. Horio, H. Hotani, Visualization of the dynamic instability of individual microtubules by dark-field microscopy, Nature 321 (1986) 605, https://doi.org/10.1038/321605a0.
[16] L. Kavitha, A. Muniyappan, S. Zdravković, M.V. Satarić, A. Marlewski, S. Dhamayanthi, D. Gopi, Propagation of kink–antikink pair along microtubules as a control mechanism for polymerization and depolymerization processes, Chin. Phys. B 23 (9) (2014) 098703, https://doi.org/10.1088/1674-1056/23/9/098703.
[17] R. Melki, M.F. Carlier, D. Pantaloni, S.N. Timasheff, Cold depolymerization of microtubules to double rings: geometric stabilization of assemblies, Biochem. 28 (1989) 9143, https://doi.org/10.1021/bi00449a028;
S.N. Timasheff, R. Melki, M.F. Carlier, D. Pantaloni, The geometric control of tubulin assemblies: cold depolymerization of microtubules into double rings, J. Cell Biol. 107 (1988) 243.
[18] S. Rasmussen, H. Karamporsala, R. Vaidyanath, K. Jensen, S.R. Hameroff, Computational connectionism within neurons: a model of cytoskeletal automata subserving neural networks, Physica D 42 (1990) 428, https://doi.org/10.1016/0167-2789(90)90093-5.
[19] H. Athenstaedt, Pyroelectric and piezoelectric properties of vertebrates, Ann. N.Y. Acad. Sci. 238 (1974) 68, https://doi.org/10.1111/j.1749-6632.1974.tb26780.x.
[20] L. Margulis, L. To, D. Chase, Microtubules in Prokaryotes: universally involved in mitosis and motility in eukaryotes, microtubules are seen in spirochetes, Science 200 (1978) 1118, https://doi.org/10.1126/science.349692.
[21] J. Jaber, R. Portugal, L.P. Rosa, Information processing in brain microtubules, Biosystems 83 (2006) 1, https://doi.org/10.1016/j.biosystems.2005.06.011.
[22] S. Zdravković, S. Zeković, A.N. Bugay, M.V. Satarić, Localized modulated waves and longitudinal model of microtubules, Appl. Math. Comput. 285 (2016) 248, https://doi.org/10.1016/j.amc.2016.03.019.
[23] A. Vinckier, C. Dumortier, Y. Engelborghs, L. Hellemans, Dynamical and mechanical study of immobilized microtubules with atomic force microscopy, J. Vac. Sci. Technol., B Microelectron. Nanometer Struct. Process. Meas. Phenom. 14 (1996) 1427, https://doi.org/10.1116/1.589113.
[24] A. Marx, E. Mandelkow, A model of microtubule oscillations, Eur. Biophys. J. 22 (1994) 405, https://doi.org/10.1007/BF00180162.
[25] S. Zdravković, M.V. Satarić, A. Maluckov, A. BalaŽ, A nonlinear model of the dynamics of radial dislocations in microtubules, Appl. Math. Comput. 237 (2014) 227, https://doi.org/10.1016/j.amc.2014.03.113.
[26] S. Zdravković, L. Kavitha, M.V. Satarić, S. Zeković, J. Petrović, Modified extended tanh-function method and nonlinear dynamics of microtubules, Chaos Solitons Fractals 45 (2012) 1378, https://doi.org/10.1016/j.chaos.2012.07.009.
[27] S. Zdravković, G. Gligorić, Kinks and bell-type solitons in microtubules, Chaos 26 (2016) 063101, https://doi.org/10.1063/1.4953011.
[28] S. Zdravković, A. Malukov, M. Dekić, S. Kuzmanović, M.V. Satarić, Are microtubules discrete or continuum systems?, Appl. Math. Comput. 242 (2014) 353, https://doi.org/10.1016/j.amc.2014.05.068.
[29] S. Zeković, A. Muniyappan, S. Zdravković, L. Kavitha, Employment of Jacobian elliptic functions for solving problems in nonlinear dynamics of microtubules, Chin. Phys. B 23 (2014) 020504, https://doi.org/10.1088/1674-1056/23/2/020504.
[30] J.A. Tuszyński, E.J. Carpenter, J.T. Huzil, W. Malinski, T. Luchko, R.F. Ludeña, The evolution of the structure of tubulin and its potential consequences for the role and function of microtubules in cells and embryos, Int. J. Dev. Biol. 50 (2006) 341, https://doi.org/10.1387/ijdb.052063jt.
[31] P. Guemkam Ghomsi, J.T. Tameh Berinyoh, F.M. Moukam Kakmeni, Ionic wave propagation and collision in an excitable circuit model of microtubules, Chaos 28 (2018) 023106, https://doi.org/10.1063/1.5001066.
[32] M.V. Satarić, D. Sekulić, M. Živanov, Solitonic ionic currents along microtubules, J. Comput. Theor. Nanosci. 7 (2010) 2281, https://doi.org/10.1166/jctn.2010.1609.
[33] F.T. Ndjomatchoua, C. Tchawoua, F.M. Moukam Kakmeni, B.P. Le Ru, H.E.Z. Tonnang, Waves transmission and amplification in an electrical model of microtubules, Chaos 6 (2016) 053111, https://doi.org/10.1063/1.4952573.
[34] S. Zdravković, M.V. Satarić, S. Zeković, Nonlinear dynamics of microtubules - a longitudinal model, Europhys. Lett. 102 (2013) 38002, https://doi.org/10.1209/0295-5075/102/38002.
[35] S.K. Liu, S.D. Liu, Nonlinear Equations in Physics, Peking University Press, Beijing, 2000.
[36] S. Zdravković, S. Zeković, A.N. Bugay, J. Petrović, Two component model of microtubules and continuum approximation, Chaos Solitons Fractals 152 (2021) 111352, https://doi.org/10.1016/j.chaos.2021.111352.
[37] S. Zdravković, D. Chevizovich, A.N. Bugay, A. Maluckov, Stationary solitary and kink solutions in the helicoidal Peyrard-Bishop model of DNA molecule, Chaos 29 (5) (2019) 053118, https://doi.org/10.1063/1.5090962.
[38] E. Fan, Extended tanh-function method and its applications to nonlinear equations, Phys. Lett. A 277 (4–5) (2000) 212–218, https://doi.org/10.1016/S0375-9601(00)00725-8.
[39] D. Ranković, Vladimir Sivčević, A. Batova, S. Zdravković, Three kinds of W-potentials in nonlinear biophysics of microtubules, Chaos Solitons Fractals 170 (2023) 113345, https://doi.org/10.1016/j.chaos.2023.113345.
[40] S. Zdravković, A.N. Bugay, A.Y. Parkhomenko, Application of Morse potential in nonlinear dynamics of microtubules, Nonlinear Dyn. 90 (2017) 2841–2849, https://doi.org/10.1007/s11071-017-3845-y.
[41] D.L. Sekulić, M.V. Satarić, M.B. Živanov, Symbolic computation of some new nonlinear partial differential equations of nanobiosciences using modified extended tanh-function method, Appl. Math. Comput. 218 (2011) 3499–3506, https://doi.org/10.1016/j.amc.2011.08.096.

[42] A.H.A. Ali, The modified extended tanh-function method for solving coupled MKdV and coupled Hirota–Satsuma coupled KdV equations, Phys. Lett. A 363 (5–6) (2007) 420–425, https://doi.org/10.1016/j.physleta.2006.11.076.
[43] C. Dai, J. Zhang, Jacobian elliptic function method for nonlinear differential-difference equations, Chaos Solitons Fractals 27 (4) (2006) 1042–1047, https://doi.org/10.1016/j.chaos.2005.04.071.
[44] O. Cornejo-Perez, J. Negro, L.M. Nieto, H.C. Rosu, Traveling-wave solutions for Korteweg–de Vries–Burgers equations through factorizations, Found. Phys. 36 (2006) 1587–1599, https://doi.org/10.1007/s10701-006-9069-5.
[45] W. Alka, A. Goyal, C.N. Kumar, Nonlinear dynamics of DNA – Riccati generalized solitary wave solutions, Phys. Lett. A 375 (3) (2011) 480–483, https://doi.org/10.1016/j.physleta.2010.11.017.
[46] N.A. Kudryashov, Simplest equation method to look for exact solutions of nonlinear differential equations, Chaos Solitons Fractals 24 (5) (2005) 1217–1231, https://doi.org/10.1016/j.chaos.2004.09.109.
[47] N.A. Kudryashov, N.B. Loguinova, Extended simplest equation method for nonlinear differential equations, Appl. Math. Comput. 205 (1) (2008) 396–402, https://doi.org/10.1016/j.amc.2008.08.019.
[48] X.-H. Wu, J.-H. He, Solitary solutions, periodic solutions and compacton-like solutions using the Exp-function method, Comput. Math. Appl. 54 (7–8) (2007) 966–986, https://doi.org/10.1016/j.camwa.2006.12.041;
J.-H. He, X.-H. Wu, Exp-function method for nonlinear wave equations, Chaos Solitons Fractals 30 (3) (2006) 700–708, https://doi.org/10.1016/j.chaos.2006.03.020.
[49] M.N. Alam, M.G. Hafez, M.A. Akbar, H.O. Roshid, Exact solutions to the (2+1)-dimensional boussinesq equation via exp($\Phi(\eta)$)-expansion method, J. Sci. Res. 7 (3) (2015) 1–10, https://doi.org/10.3329/jsr.v7i3.17954.
[50] M.N. Alam, F.B.M. Belgacem, Microtubules nonlinear models dynamics investigations through the exp($\Phi(\xi)$)-expansion method implementation, Mathematics 4 (6) (2016) 1–13, https://doi.org/10.3390/math4010006.
[51] H.-M. Fu, Z.-D. Dai, Double exp-function method and application, Int. J. Nonlinear Sci. Numer. Simul. 10 (7) (2009) 927–934, https://doi.org/10.1515/IJNSNS.2009.10.7.927.
[52] W.-X. Ma, T. Huang, Y. Zhang, A multiple exp-function method for nonlinear differential equations and its application, Phys. Scr. 82 (6) (2010) 065003, https://doi.org/10.1088/0031-8949/82/06/065003.
[53] K.K. Ali, C. Cattani, J.F. Gómez-Aguilar, D. Baleanu, M.S. Osman, Analytical and numerical study of the DNA dynamics arising in oscillator-chain of Peyrard-Bishop model, Chaos Solitons Fractals 139 (2020) 110089, https://doi.org/10.1016/j.chaos.2020.110089.
[54] P.F. Byrd, M.D. Friedman, Handbook of Elliptic Integrals for Engineers and Scientists, 2nd ed., Springer Berlin, Heidelberg GMBH, 1971.
[55] N.I. Akhiezer, Elements of the Theory of Elliptic Functions, New Ed edition, Translations of Mathematical Monographs, vol. 79, American Mathematical Society, Providence, 1990.
[56] A.J.M. Jawad, M.D. Petković, A. Biswas, Modified simple equation method for nonlinear evolution equations, Appl. Math. Comput. 217 (2010) 869–877, https://doi.org/10.1016/j.amc.2010.06.030.
[57] S. Zdravković, S. Zeković, Nonlinear dynamics of microtubules and series expansion unknown function method, Chin. J. Phys. 55 (6) (2017) 2400–2406, https://doi.org/10.1016/j.cjph.2017.10.009.
[58] D. Chretien, S.D. Fuller, E. Karsenti, Structure of growing microtubule ends: two-dimensional sheets close into tubes at variable rates, J. Cell Biol. 129 (1995) 1311, https://doi.org/10.1083/jcb.129.5.1311.
[59] R.B. Dye, S.P. Fink, R.C.J. Williams, Taxol-induced flexibility of microtubules and its reversal by MAP-2 and Tau, J. Biol. Chem. 268 (1993) 6847, https://doi.org/10.1016/S0021-9258(18)53113-6.
[60] F. Gittes, B. Mickey, J. Nettleton, J. Howard, Flexural rigidity of microtubules and actin filaments measured from thermal fluctuations in shape, J. Cell Biol. 120 (1993) 923, https://doi.org/10.1083/jcb.120.4.923.
[61] H. Athenstaed, Pyroelectric and piezoelectric properties of vertebrates, Ann. N.Y. Acad. Sci. 238 (68) (1974), https://doi.org/10.1111/j.1749-6632.1974.tb26780.x.
[62] M.V. Satarić, J.A. Tuszyński, Nonlinear dynamics of microtubules: biophysical implications, J. Biol. Phys. 31 (2005) 487, https://doi.org/10.1007/s10867-005-7288-1.
[63] M.V. Satarić, J.A. Tuszyński, Relationship between the nonlinear ferroelectric and liquid crystal models for microtubules, Phys. Rev. E 67 (2003) 011901, https://doi.org/10.1103/PhysRevE.67.011901.
[64] E.M. Mandelkow, E. Mandelkow, R.A. Milligan, Microtubule dynamics and microtubule caps: a time-resolved cryo-electron microscopy study, J. Cell Biol. 114 (5) (1991) 977–991, https://doi.org/10.1083/jcb.114.5.977.
[65] A.M. Samsonov, Strains Solitons in Solids and How to Construct Them, Monographs and Surveys in Pure and Applied Mathematics, vol. 117, Chapman and Hall/CRC, CRC Press, 2001.
[66] A.M. Samsonov, On some exact travelling wave solutions for nonlinear hyperbolic equations in nonlinear waves and dissipative effects, edited by D. Fusco and A. Jeffrey, Pitman Res. Notes Math. Ser. (1991).
[67] Z.X. Wang, D.R. Guo, Special Functions, World Scientific, Singapore, 1989.
[68] E.T. Whittaker, G.N. Watson, A Course of Modern Analysis, 4th edition, Cambridge University Press, Cambridge, 1996.
[69] R. Beals, R. Wong, Special Functions, Cambridge University Press, Cambridge, 2010.
[70] H. Stebbins, C. Hunt, The nature of the clear zone around microtubules, Cell Tissue Res. 227 (1982) 609, https://doi.org/10.1007/BF00204791.
[71] H. Fröhlich, Modern bioelectrochemistry, in: F. Gutmann, H. Keyzer (Eds.), 1st edition, Springer New York, New York, 1986.
[72] J.E. Schoutens, Dipole-dipole interactions in microtubules, J. Biol. Phys. 31 (2005) 35, https://doi.org/10.1007/s10867-005-3886-1.
[73] S.E. Mkam Tchouobiap, H. Mashiyama, Quasiharmonic approximation for a double Morse-type local potential model: application to a H2PO4-type phase diagram, Phys. Rev. B 76 (2007) 014101, https://doi.org/10.1103/PhysRevB.76.014101.
[74] E. Nogales, M. Whittaker, R.A. Milligan, K.H. Downing, High-resolution model of the microtubule, Cell 96 (1999) 79, https://doi.org/10.1016/S0092-8674(00)80961-7.
[75] S. Zdravković, M.V. Satarić, V. Sivčević, General model of microtubules, Nonlinear Dyn. 92 (479) (2018), https://doi.org/10.1007/s11071-018-4069-5.
[76] D. Ranković, Slobodan Zdravković, Two component model of microtubules - subsonic and supersonic solitary waves, Chaos Solitons Fractals 164 (2022) 112693, https://doi.org/10.1016/j.chaos.2022.112693.
[77] L.A. Amos, D. Schlieper, Microtubules and maps, Adv. Protein Chem. 71 (2005) 257–298, https://doi.org/10.1016/S0065-3233(04)71007-4.
[78] D.L. Sekulić, M.V. Satarić, M.B. Živanov, Symbolic computation of some new nonlinear partial differential equations of nanobiosciences using modified extended tanh-function method, Appl. Math. Comput. 218 (2011) 3499, https://doi.org/10.1016/j.amc.2011.08.096.
[79] C.V. Sindelar, K.H. Downing, An atomic-level mechanism for activation of the kinesin molecular motors, Proc. Natl. Acad. Sci. USA 107 (2010) 4111, https://doi.org/10.1073/pnas.0911208107.
[80] J. Fabera, R. Portugala, L. Pinguelli Rosa, Information processing in brain microtubules, Biosystems 83 (2006) 1, https://doi.org/10.1016/j.biosystems.2005.06.011.
[81] S. Flacha, A.V. Gorbach, Discrete breathers - advances in theory and applications, Phys. Rep. 467 (2008) 1, https://doi.org/10.1016/j.physrep.2008.05.002.
[82] E. Fan, Extended tanh-function method and its applications to nonlinear equations, Phys. Lett. A 277 (2000) 212, https://doi.org/10.1016/S0375-9601(00)00725-8.

[83] L. Kavitha, N. Akila, A. Prabhua, O. Kuzmanovska-Barandovska, D. Gopi, Exact solitary solutions of an inhomogeneous modified nonlinear Schrödinger equation with competing nonlinearities, Math. Comput. Model. 53 (2011) 1095, https://doi.org/10.1016/j.mcm.2010.10.030.
[84] S. Huang, D.E. Ingber, The structural and mechanical complexity of cell-growth control, Nat. Cell Biol. 1 (1999) E131, https://doi.org/10.1038/13043.
[85] H. Salman, Y. Gil, R. Granek, M. Elbaum, Microtubules, motor proteins, and anomalous mean squared displacements, Chem. Phys. 284 (2002) 389, https://doi.org/10.1016/S0301-0104(02)00669-9.
[86] M. Cifra, J. Pokorny, D. Havelka, O. Kućera, Electric field generated by axial longitudinal vibration modes of microtubule, Biosystems 100 (2010) 122, https://doi.org/10.1016/j.biosystems.2010.02.007.
[87] J.A. Tuszyński, B. Trpisová, D. Sept, M.V. Satarić, The enigma of microtubules and their self-organizing behavior in the cytoskeleton, Biosystems 42 (1997) 153, https://doi.org/10.1016/S0303-2647(97)01704-8.
[88] M.V. Satarić, L. Budinski-Petković, I. Lončarević, J.A. Tuszyńsky, Modelling the role of intrinsic electric fields in microtubules as an additional control mechanism of bi-directional intracellular transport, Cell Biochem. Biophys. 52 (2008) 113, https://doi.org/10.1007/s12013-008-9028-1.
[89] W.O. Hancock, Intracellular transport: kinesins working together, Curr. Biol. 18 (2008) R715, https://doi.org/10.1016/j.cub.2008.07.068.
[90] S.P. Gross, M. Vershinin, G.T. Shubeita, Cargo Transport: two motors are sometimes better than one, Curr. Biol. 17 (2007) R478, https://doi.org/10.1016/j.cub.2007.04.025.
[91] K.C. Chou, C.T. Zhang, G.M. Maggiora, Solitary wave dynamics as a mechanism for explaining the internal motion during microtubule growth, 1994 Biopolymers: Orig. Res. Biomolec. 34 (1) (1994) 143–153, https://doi.org/10.1002/bip.360340114.
[92] A.M. Gomez, B.G. Kerfant, G. Vasort, Microtubule disruption modulates Ca^{2+} signaling in rat cardiac myocytes, Circ. Res. 86 (2000) 30, https://doi.org/10.1161/01.RES.86.1.30.